The changes in precipitation characteristics during the Baiu (Mei-yu) season of the global warming climate simulated by a cloud-resolving non-hydrostatic regional model

*Kazuaki YASUNAGA[1], Yasutaka WAKAZUKI[1], Masanori YOSHIZAKI[2], Chiashi MUROI[2], Kazuo KURIHARA[2], Akihiro HASHIMOTO[1], Sachie KANADA[1], Teruyuki KATO[2]

[1]*Advanced Earth Science and Technology Organization, Tokyo*
[2]*Meteorological Research Institute / Japan Meteorological Agency, Tsukuba*

1. Introduction

We are trying to predict climate changes over East Asia during the rainy season in early summer (Baiu season), when greenhouse gas concentrations in the atmosphere increase, making use of a high-resolution nonhydrostatic model nested into a 20km-mesh AGCM.

Our previous paper (Yoshizaki et al. 2005) showed the precipitation during the Baiu season increases over the southern Japan islands, and decreases over the northern Japan Islands and the northern Korean Peninsula. It was also presented that the frequency of occurrence of heavy rainfall greater than 30 mm h^{-1} increases over the Japan Islands. However, there are two possibilities for the increase in the rainfall amounts and heavy rainfall frequency around the southern Japan islands in the warming climate simulation; (1) the Baiu front is long sustained in the warming climate simulation, or (2) precipitation characteristics associated with the Baiu front is changed. Therefore, in the present study, the changes of precipitation characteristics over East Asia are examined.

2. Model descriptions and experimental designs

A nonhydrostatic model named JMA-NHM, which has been jointly developed by the Meteorological Research Institute and the Numerical Prediction Division, Japan Meteorological Agency, is employed as a regional climate model. The JMA-NHM has been utilized for short-term predictions and climate simulation, and good model performances have been confirmed, especially for the forecast of heavy rainfall (Wakatsuki et al. 2004). The JMA-NHM is detailed in Saito et al. (2001).

The horizontal grid size of the regional climate model is 5 km, and the domain covers an area of 4000 km x 3000 km (Fig. 1). The model has 48 layers in the stretched vertical, with the finest resolution (20m) near the surface, and the coarsest resolution (920m) at the model top. Rayleigh damping is imposed near the upper boundary. Although a horizontal grid of 5 km can not fully resolve convective updrafts, the JMA-NHM with a horizontal grid of 5 km has successfully reproduced many heavy rainfall events, making use of explicitly represented cloud microphysics only (e.g., Kato 1998, Kato and Goda 2001). Therefore, no convective parameterization is used in the present study.

*Corresponding author address: Kazuaki Yasunaga, Meteorological Research Institute, 1-1 Nagamine, Tsukuba, Ibaraki 305-0052 Japan: e-mail: kyasunag@mri-jma.go.jp

The initial and lateral boundary conditions of the regional climate model, JMA-NHM were obtained from the outputs of the AGCM. In order to couple the AGCM and NHM smoothly, a spectral boundary coupling (SBC) method was adopted (Kida et al. 1991; Yasunaga et al. 2004). The SBC method is applied to the fields of horizontal winds and temperature above a height of 5km every 20 minutes. The SST is same as used in the AGCM. Since our goal is to predict climate changes during the Baiu season around East Asia, the simulation period is set as June and July.

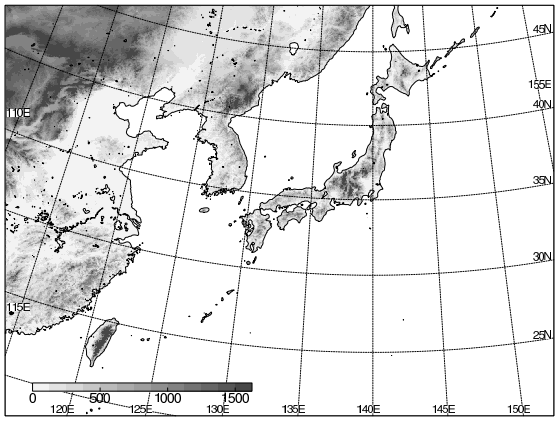

Fig. 1: The domain and orography of the JMA-NHM.

3. Results

Figure 2 represents accumulated rainfall amounts and normalized frequencies of precipitation over the model domain in June and July. The first 10 days data and data within 500 km of the nearest boundary are excluded in order to remove the influence of the initial fields and lateral boundary. While the rainfall amounts in June of the warming climate simulation agree with those in the present climate simulation, more rainfall is brought about in July of the warming climate simulation (Fig. 2a). The frequency of precipitation in the warm climate simulation greatly increases from that in the present climate simulation with intensity of the rainfall in July, although there are little differences in precipitation frequencies in June of between the present and warming climate (Fig. 2b).

In order to investigate how large precipitation systems mainly bring about rainfall over East Asia during June and July, the precipitation systems are classified according to area of the system (Fig. 3). The area of a precipitation system is calculated from aggregates of

precipitation grids connected with each other to north-south or east-west directions. The precipitation grid is defined as the intensity of the rainfall greater than 1 mm hr^{-1}. In this analysis, hourly outputs are used, and the continuity between the outputs is not considered.

Number of the precipitation system in the warm climate simulation agrees with that in the present climate simulation during June and July, except for that with the area of lager than 90000 km^2 in July (Fig. 3a). The precipitation systems with the lager area bring about more rainfall in June (Fig. 3b). There is also a large difference in the rainfall amounts from the precipitation systems with the area of lager than 90000 km^2 in July of the present and warming climate simulations (Fig. 3b). The precipitation systems with the area of lager than 90000 km^2 more frequently develop, and lead to more rainfall amounts in July in the warming climate than in the present climate. Moreover, it can be thought that the increase of the precipitation systems with the area of lager than 90000 km^2 results in the increase of the heavy rainfall event in July of the warming climate (Fig. 2b).

The precipitation systems with the area of lager than 90000 km^2 are most frequently observed around 30-40° N, 127-138° E in July of the warm climate (not shown). These precipitation systems are classified into sub-synoptic or meso-alpha-scale cloud systems, which are associated with relevant cyclonic circulation systems. The baroclinicity is deeply connected with the development of the cyclonic circulation systems, although condensation heating also plays the important role. The north-south gradient of the equivalent potential temperature around 30-40° N, 127-138° E is steeper in July of the warm climate than that in July of the present climate (not shown). The stronger baroclinicity in July of the warm climate simulation is consistent to the increase of the precipitation systems with the area of lager than 90000 km^2.

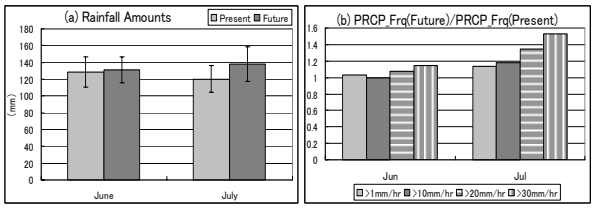

Fig.2: (a) Accumulated rainfall amounts, and (b) precipitation frequency in the warming climate normalized by that in the present climate over the model domain in June and July. In (a), light and dark gray columns denote the results in the present and warming climate simulation, respectively. Vertical lines show ranges within one standard deviation. In (b), light gray, dark gray, lateral stripe, and vertical stripe columns denote the normalized frequency of precipitation with the intensity of the rainfall greater than certain thresholds (1 mm hr^{-1},10 mm hr^{-1}, 20 mm hr^{-1}, and 30 mm hr^{-1}), respectively.

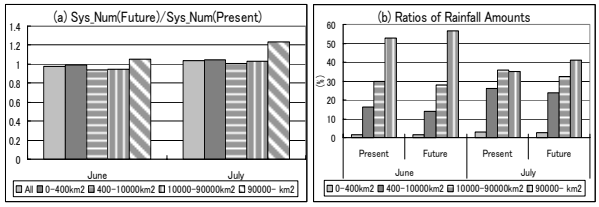

Fig.3: (a) Number of the precipitation systems with the certain size in the warming climate normalized by that in the present climate, and (b) ratios of the rainfall amounts brought about by the precipitation systems with the certain area to total rainfall amounts over the model domain in June and July. In (a), light gray, dark gray, lateral stripe, vertical stripe, and slanting stripe columns denote the normalized number of all precipitation systems and the systems with the area of 0-400 km^2, 400-10000 km^2, 10000-90000 km^2, and 90000- km^2, respectively. In (b), light gray, dark gray, lateral stripe, vertical stripe also show the ratios of the rainfall amounts from the precipitation systems with the area of 0-400 km^2, 400-10000 km^2, 10000-90000 km^2, and 90000- km^2, respectively.

Acknowledgements

This study is conducted by the fund of Research Revolution 2002, and the numerical calculations are made by NEC SX-6 on Earth Simulator.

References

[1]Deardorff, J. W., 1980: Numerical investigation of neutral and unstable planetary boundary layers. *Boundary-Layer Meteorol.*, **18**, 495-527.

[2]Kato, T., 1998: Numerical simulation of the band-shaped torrential rain observed over southern Kyushu, Japan on 1 August 1993. *J. Meteor. Soc. Japan*, **76**, 97-128.

[3]Kato, and Goda, 2001: Formation and Maintenance Processes of a Stationary Band-shaped Heavy Rainfall Observed in Niigata on 4 August 1998. *J. Meteor. Soc. Japan*, **79**, 899-924.

[4]Saito, K., T. Kato, H. Eito and C. Muroi, 2001: Documentation of the Meteorological Research Institute / Numerical Prediction Division Unified Nonhydrostatic Model. *Tech. Rep.of MRI*, **42**, p133.

[5]Wakazuki, Y. et al. 2004: Numerical experiment of climate change caused by global warming with the 5-km horizontal grid non-hydrostatic regional model. (2) Evaluation of the prediction accuracy and heavy rainfall frequency (in Japanese). *Prep. Autumn Meeting Meteor. Soc. Japan*, **86**, 147.

[6]Yasunaga, K., H. Sasaki, Y. Wakazuki, T. Kato, C. Muroi, A. Hashimoto, S. Kanada, K. Kurihara, M. Yoshizaki and Y. Sato, 2004a: Performance of the long-term integrations of the Japan Meteorological Agency nonhydrostatic model with use of the spectral boundary coupling method. Submitted to *Weather and Forecasting*.

[7]Yoshizaki, M. et. al. 2005: Changes of Baiu (Mei-yu) frontal activity in the global warming climate simulated by a cloud-resolving non-hydrostatic regional model. *SOLA* (*submitted*)